Informes Técnicos Ciemat 1013
Febrero, 2003

Edge and Plasma-Wall Interaction Diagnostics in the TJ-II Stellarator

F.L. Tabarés
D. Tafalla
B. Brañas
A. Hidalgo
I. García-Cortés
A. López-Fraguas
P. Ortiz

Asociación EURATOM/CIEMAT para Fusión - 83

Departamento de Fusión y Física de Partículas Elementales

Toda correspondenica en relación con este trabajo debe dirigirse al Servicio de Información y Documentación, Centro de Investigaciones Energéticas, Medioambientales y Tecnológicas, Ciudad Universitaria, 28040-MADRID, ESPAÑA.

Las solicitudes de ejemplares deben dirigirse a este mismo Servicio.

Los descriptores se han seleccionado del Thesauro del DOE para describir las materias que contiene este informe con vistas a su recuperación. La catalogación se ha hecho utilizando el documento DOE/TIC-4602 (Rev. 1) Descriptive Cataloguing On-Line, y la clasificación de acuerdo con el documento DOE/TIC.4584-R7 Subject Categories and Scope publicados por el Office of Scientific and Technical Information del Departamento de Energía de los Estdos Unidos.

Depósito Legal: M -14226-1995
ISSN: 1135 - 9420
NIPO: 402-03-005-6

Editorial CIEMAT

CLASIFICACIÓN DOE Y DESCRIPTORES

S44; S70

ATOMIC BEAMS; LASERS; PLASMA DIAGNOSTICS; PLASMA INSTABILITIES; EDGE LOCALIZED MODES; TOKAMAK DEVICES; STELLARATORS

Edge and Plasma-Wall Interaction Diagnostics in the TJ-II Stellarator

Tabarés, F.L.; Tafalla, D.; Brañas, B.; Hidalgo, A.; García-Cortés, I.;
López-Fraguas, A.; Ortiz, P.

24 pp. 8 figs. 17 refs.

Abstract

The operation of the TJ-II stellarator, carriedout under ECR heating condtions until novv, has implieda careful control of partid e sources and the associated plasma-wall interaction processes. A clear coupling betvveen the plasma edge parameters and those processes has been identified, Therefore, an important effort has been devoted to the development of dedcated dagnostics in both fields. Remarkable success has been attained in the development of atomic-beam based edge dagnostics, namely, thermal Li and supersonic He beams. In particular, fast (up to 200 Hz) sampling of temperature and density profiles has been made possible through an upgraded versión of the pulsed, supersonic He beam dagnostic. In this paper, vvork devoted to the upgradng of these techniques is described Also, preliminary experiments oriented to the validation of the collisional radative models usedin the beam-based dagnostic interpretaron as well as simulations of Láser Induced Fluorescence (LIF) studes of level populations of electronically excited He atoms are shovvn.

Diagnósticos de la Interacción Plasma Pared y del Borde del Plasma en el Stellarator TJ-II

Tabarés, F.L.; Tafalla, D.; Brañas, B.; Hidalgo, A.; García-Cortés, I.;
López-Fraguas, A.; Ortiz, P.

24 pp. 8 figs. 17 refs.

Resumen

La operación del TJ-II se ha realizado hasta la fecha por calentamiento ECRH y ha implicado el control riguroso de las fuentes de partículas y de los procesos de interacción entre el plasma y la primera pared Dado el fuerte acoplo existente entre los parámetros de la zona periférica del plasma y los procesos de interacción plasma-pared, se ha llevado a cabo un esfuerzo considerable en el dagnóstico de ambos aspectos del problema. En particular, se ha conseguido un avance muy notable en el desarrollo de los diagnósticos basados en haces atómicos, como son el de Li térmico y el de He supersónico. Respecto a este ultimo, se ha desarrollado un método para su utilización a frecuencias de repetición de hasta 200 Hz para la medda cuasi-continua de los perfiles de densidad y temperatura electrónicas. En el presente trabajo se describen las mejoras realizadas en estos diagnósticos. También se describen los resultados preliminares obtenidos respecto a la validación del modelo Colisional-Radativo (C-R) usado en la interpretación de los datos del haz de He así como la simulación de los experimentos de Fluorescencia Inducida por Láser (LIF) orientados a la medda directa de las poblaciones de estados excitados implicadas en el modelo C-R.

1. Introduction: The TJ-II device, a four period, helical axis stellarator with <a>=25 to 10cm, R=1.5 m, B_T (0)< 1T, has been operated under ECRH heating conditions, producing plasmas with Te (0) up to 2 keV, at densities limited by the cut-off limit of ne (0)<$1.7.10^{19}$ m^{-3} [1]. The high-injected power, up to 600 kW, and the proximity of the walls to the plasma make plasma-wall interaction processes extremely critical for the plasma operation [2]. Therefore, an important effort has been devoted to the characterisation of these phenomena and their relation with edge parameters. Particle control, rather than radiated power, appeared as the main challenge under typical conditions, arising from the relatively large inner surface/ plasma volume ratio and low cut-off value [3]. For that purpose, mass spectrometry, optical spectroscopy and fast (~1 millisecond) fuel injection monitors were applied to the studies of particle inventory.
Systematic plasma edge studies have been undertaken for global transport characterisation. For that purpose, Langmuir probes [4], either fixed to the limiter or fast reciprocating, and a set of atomic beam diagnostics [5], which includes thermal (Li) and supersonic (He) ones, has been implemented. These beams have been upgraded in the last years in order to cope with new operational regimes of TJ-II. In addition, testing of the model assumptions implicit in the usual interpretation [6,7] of these diagnostics has been addressed. In such respect, the Laser Induced Fluorescence technique is being incorporated in order to validate the collisional-radiative (CR) model use to date for the He beam diagnostic. In the present work, a description of the different TJ-II edge and plasma-wall diagnostics, their achievements and upgrading is given.

2. Plasma-wall interaction diagnostics:

The main features of the plasma-wall interaction pattern and SOL characteristics of the TJ-II plasmas have been previously described [4,8]. Briefly, the last closed flux surface (LCFS) can in principle be defined by the intersection of the field lines with the part of the vessel surrounding the central helical coil, which acts as a helical limiter, or by two poloidal, movable limiters [4]. These limiters have been recently modified for compatibility with the low Z scenario required for the NBI heated plasmas. Their shape is designed to adjust to the plasma boundary for most the magnetic configurations with large volumes, the cases suitable to NBI heating. An additional toroidal shaping aiming to smooth the power deposition on the limiters was performed assuming an exponential profile for the ion fluxes in the SOL. Hence the limiting surface of the limiters has the form of a saddle, as shown in Fig. 1. Each limiter is made of a graphite block (fine grain, pyrolytic, Shunk FU4206) mounted on an SS plate. They are located in the inferior ports of the sectors A3 and C3. The remotely controlled support mechanism allows a vertical displacement in order to match the desired position with respect to the plasma. The normal functioning mode in the NBI heating operation will be to set the

limiters just inside the LCMS to reduce the thermal loads from the heated plasma to the vacuum chamber. This critical position is very dependent on the magnetic configuration.

In order to characterize the SOL (Scrape-off Layer) plasma profiles we have installed Langmuir probe sets distributed along the two limiters, in the poloidal and toroidal direction. Each set is made of four single tungsten tips with a diameter of 0.9 mm and 3 mm of length, thus giving fairly good radial resolution. Aside from floating potential and ion saturation current, each set is able to measure temperature and density by a triple probe configuration in a small plasma volume (9 mm^2 x 3 mm). The Fig.1shows the toroidal and poloidal locations where the set of Langmuir probes are embedded. Note that the probe array with toroidal distribution in Fig. 1 gives, due to the limiter design, a SOL radial profile of the plasma parameters with a radial separation between probes about 2.5 mm. The signals are digitalized to high frequency sample rate (100 kHz) to evaluate fluctuations of different magnitudes and ExB turbulent transport in the SOL plasma. An estimation of the power deposition at the limiters in the NBI phase of the machine and possible poloidal and toroidal asymmetries in the SOL can be studied in detail with this distribution of Langmuir probes. A couple of thermoresistances (PT100) are embedded in the backside. Also, a gas injection manifold has been installed in the central part of both limiters for gas screening studies. In additions, the insertion of the limiters into the plasma has been motorised in order to allow for remote control of their position. A CCD video camera, provided with a set of interference filters, is focussed from a toroidal window to check for impurity production and particle recycling patterns. In addition, V and UV spectroscopy is applied elsewhere in the plasma [9].

As mentioned above, particle inventory control has been somehow problematic in the ECRH campaign. A differentially pumped mass spectrometer is systematically used for outgassing studies. As an example, figure 2 shows the impact of the outgassing of He from the stainless steel wall in the density control during operation of TJ-II with H plasmas. Mass spectrometry, directly coupled into the vacuum vessel, was also used to characterise the wall state before operation by thermal desorption induced by the focussed MW beam into the helical groove. Finally, the flow of gas injected during the discharge is monitored with a fast time response by using a simple gas injection system (GIS) design (Fig.3a). The transient pressure generated in a reservoir (buffer) inserted in the way from the piezo valve to the vacuum vessel is detected by a fast capacitance manometer (MKS, 1 ms time response, 1 mbar range). A total time constant of 2-3 ms is typically attained. Calibration of the system is easily performed by static expansion into the calibrated buffer volume. In addition to the speed, the system is insensitive to the stray magnetic field and the type of gas. Figure 3b shows an example of the response of some typical traces to the injection of a short gas pulse in TJ-II at the beginning of the discharge. Some of the main features of the GIS are readily seen in the figure, such as the almost parallel response of the Ha puffing monitor (i.e., plasma edge

emission) and the shape of the gas pulse waveform as recorded by the capacitance manometer. Also, the quick rise in the line density corresponds to a fuelling efficiency (n_e'/Q) of f ~ 0.25.

3. Edge/SOL diagnostics:

A fast reciprocating probe has been operative in TJ-II almost from the beginning of its operation [10]. The probe can be inserted into the plasma edge region from the top of TJ-II at a velocity of ~1m/s up to 3 cm inside the LCFS. In the last year, the probe head has been adapted as a Mach probe. Results on Mach number profiles and the presence of configuration-dependent shears in the TJ-II toroidal flows will be presented elsewhere [11]

The thermal Li beam [5] is generated into a cylindrical oven surrounded by an electrical resistance, which heats it up to temperatures in the range 590-630 °C. The oven is located on a top window of the machine (see fig.4) and the beam is directed downwards with an angle of 22° with respect to the vertical. This angle can be changed to adapt the beam line to the different plasma configuration. The system is differentially pumped to a base pressure of < 1.10^{-7} mbar (<1.10^{-5} during operation). In its previous design, problems arising from the condensation of the Li efflux into the intermediate duct were found. Although a copper cylinder was installed to isolate the effusive beam from the hot wall, spurious contributions to the beam from lithium evaporated outside the oven eventually happened. Also, strong gluing through molten Li of the lower lid, used to refill the oven, made the periodic refreshment of Li fairly cumbersome. In order to improve the operation of the diagnostic, new designs of the oven have been tried. First, a mechanical beam obstructer, pneumatically operated, was fixed to the 3mm nozzle, thus avoiding the continuous accumulation of Li into the duct. Secondly, two different heating designs have been tested. One of them includes radiative heating of an oversized oven, with a lid in the upper side, i.e. not reached by the molten lithium, and a vacuum break (CF gasket) on top, not directly heated by the radiator. Even with the beam continuously effusing, the high localization of the hot area prevented from periodic re-evaporation of the condensed lithium. In a second version, a small container is hung under vacuum in a dedicated chamber and directly heated by a thermocoax wire. Either of the new designs allow for a cleaner and trouble-free refilling of the Li source. In all cases, the flux of Li atoms at the observation region is ~10^{14} atoms/s and its local density is of the order of 7.10^{8} atoms/cm^3. A circular collimator of 5 mm, located at a distance of 80 cm from the observation region, define a divergence of 1° and a beam size at the measurement region (FWHM) of 1.7 cm. For the ECRH plasmas the beam has a characteristic penetration depth inside the LCFS of ≈2 cm allowing density estimation up to r/a≈0.7.

The emission from the excited Li atoms at 671 nm is collected from a lateral port by means of a lens and an interference filter (FWHM=1 nm) and recorded with a multianode photomultiplier array of 16 channels. The array output signals, after passing through a set of preamplifiers, are sampled and recorded with the standard instrumentation of the TJ-II data acquisition system. The responses of the 16 channels, including the whole detection system, were relatively calibrated *in situ*. The radial resolution is 4.5-6 mm. The alignment of beam and detection optics was made using a movable reference inserted into the vacuum chamber for that purpose. Previously to the installation on TJ-II, the beam was tested in the laboratory using a quadrupole mass spectrometer as detector of the Li atoms. The beam intensity dependence on oven temperature and gas pressure in the intermediate duct was checked.

A simulation of the propagation of a thermal Li beam into the plasma has been made using a stationary collisional-radiative model which considers five levels: the ground (2s) and the excited levels up to n=3 (2p, 3s, 3p and 3d). The attenuation is calculated for each spatial step (a resolution better than 20 μ is required to obtain good results). Recombination is neglected for the typical temperatures considered (> 10 eV). This simulation has been used to estimate the effect on the reconstruction of the density profile of considering only the ground and the 2p excited levels as well as the effect of the ionisation of the 2p state. The error due to considering only one excited state increases with density and decreases with temperature, being negligible for electronic densities lower than 4.10^{13} m^3 and Te>100 eV. This approximation leads to a overestimation of the reconstructed density values that for a typical TJ-II profile would be of the order of 10-20% at the most internal positions where the error is maximum. The effect of considering the ionisation of the 2p state increases also at low temperatures and high densities but is larger than the former. For electronic density $n_e=5.10^{18}$ m^{-3} and temperature T_e between 10 and 100 eV the effective ionisation cross section S_{ief} (that includes ionisation cross sections from the 2s state (S_i) and the 2p state (S_i^*)) is around 25% larger than S_i. Nevertheless, the reduction on the emission due to the 2p ionisation is less than 5%. Therefore, it is concluded that while the omission of the 3s, 3p and 3d states is a good approximation, the attenuation of the beam due to ionisation of the excited state must be considered for the TJ-II plasmas.

In addition these considerations, the procedure used for density profile reconstruction from the Li beam intensity takes also into account the beam acceleration by the plasma. Both the effective ionization cross-section and the mean velocity of the Li atoms vary with the position along the beam trajectory. The following expression is used:

$$n_e = \frac{I}{c_{12}\left[\int\left(\frac{S_{ief}}{c_{12}} I\left\langle\frac{1}{v}\right\rangle dr\right) - \frac{I}{A}\right]} \quad \text{with} \quad S_{ief} = S_i + S_i^* \frac{c_{12} n_e}{A + S_i^* n_e}$$

where I is the emitted intensity of the Li atoms at 671 nm, c_{12} is the 2s-2p electron impact excitation cross-section, A is the radiative de-excitation probability of the 2p excited Li atoms and v their velocity. The electron density profile is obtained through an iterative procedure. Four iterations are typically enough for convergence.

The He beam diagnostic has been described in detail previously [5,12]. Its application to the TJ-IU torsatron pioneered the use of supersonic beams in hot plasma diagnostics. The source [13] consists of a fast, pulsed piezoelectric valve with a nozzle of 0.3 mm diameter and a parabolic profile skimmer with a diameter of 0.5 mm. The nozzle-skimmer distance can be varied. Using the same set-up as for the Li beam, and a manometer as detector of the He atoms, the alignment between nozzle and skimmer was optimised, and the beam geometry fully characterised. For the experiments in TJ-II a distance of 25 mm was chosen defining a divergence of 1.4°. The mean beam velocity is 1500-1750 m/s and the velocity distribution is defined by a speed ratio of 10-20, depending on source pressure [14]. Pulse duration in the experiments was 1-2 ms and He stagnation pressure was in the range 0.6-1.2 bar. The experimental set-up is shown in fig. 5. The beam is launched from a top window of TJ-II being the nozzle at 90 cm from the plasma edge. Beam diameter at the observation region is around 2.4 cm, while the flux of He atoms, based on the measurements previously mentioned is estimated to be of the order of 10^{10} cm^{-3}. The beam can also be characterised at its definitive location in the TJ-II chamber with a manometer positioned in front of it (fig.5). A velocity of 1720 m/s is inferred from time of flight of the He atoms. Simultaneous detection of the three He lines [7,14] used for reconstruction of the edge temperature and density profiles (667.2nm, 706.5 nm and 728.1 nm) is made through a set of 16- anode photomultiplier arrays with interference filters (FWHM=1 nm). The detection system is calibrated in a He glow discharge with an OMA spectrometer. The geometrical radial resolution was ~3 mm.

By using the set-up just described, at the time of the beam injection a sharp increase of the line intensities was observed, but it was followed by a weaker tail that lasted several tens of milliseconds, due to the effusion of the He gas contained in the expansion chamber of the beam source [5], as displayed in figure 6, left. This tail precluded the multipulse operation of the beam. In the last campaign, this problem has been eliminated by inserting a second chamber in series with the beam. Differential pumping is done by a 150 l/s turbo pump. As an example of the new performance, figure 6, right, shows the emission of the 706 line (triplet system) under the new geometry for several radial locations. As seen, a repetition rate as high as 200 Hz is possible now, at least for selected time periods in the discharge. The width of the pulses

in the case shown is determined by the time response of the amplifier, and, due to the monoenergetic character of the expansion, it can be made basically equal to that of the valve pulse.

Agreement among different edge diagnostics, as Li beam, probes and reflectometer is generally good [5], if one makes allowance for their relative uncertainties. Here, only the results of the He beam are compared. Figure 7 shows electron density and temperature profiles deduced from different diagnostics: He beam, and reflectometer, for ne, and He beam, ECE, and Langmuir probes for Te, for metal and boronised walls. Note the agreement in Te profiles except in the last point of ECE data (no optically thick plasma). Also, a lower value for density is deduced from the He diagnostic, even with the possible dispersion in the profile deduced from the reflectometer.

4. Test of the Collisional Radiative Model.

As it is well known, the reconstruction of the electron density and temperature profiles from the He beam diagnostic is directly linked to the application of a suitable collisional-radiative (C-R) model [6a]. Uncertainties in the relevant cross sections and lack of inclusion of all the implied species typically make the model itself the source of the largest errors in the profile reconstruction [6b]. Thus, for example, Andrew and O´Mullane showed that errors in the tabulated rate constants, which are normally within the standard experimental uncertainties, do have a direct and highly selective effect on the profile reconstruction [7]. The combination of supersonic beams and electron-heated plasmas are in principle ideally suited scenarios for testing the C-R model. First, due to their low divergence and mono-energetic characteristics, the propagation into the plasma of a supersonic beam can be drastically simplified to its radial component. Moreover, the low ion temperatures present in ECRH plasmas allows for the ion-He associated collisional processes to be neglected in the simulations. Then, although only the line ratios are normally used for the profile reconstruction, self-consistency can be checked through the simulation of the spatial distribution of all the emission lines based on the reconstructed emission profiles. Care must be taken, however, due to the possible contribution of non-thermal electrons to the excitation lines. Comparison of the inferred profiles with those obtained with other diagnostics must then be used as a test for such contribution.

As an example, figure 8 shows one of the C-R model checks in our plasmas. The experimental profiles for the three lines involved (16 points) are first smoothed and their ratios (667/728 for ne and 728/706 for Te) used for the ne and Te profile reconstruction. The resulting profiles, shown at the right are fitted into the C-R code, in its steady state approach, and the radial evolution of the lines is reconstructed. Note that the density profile shows a minimum near r/a= 0.8. This is attributed to the lack of

equilibration among the relevant levels due to the long time required at these low ne values [14]. The rate constants used in the model are those recommended by Brix [6], but the Johnson and Hinnov value [15] for the transitions with $\Delta n=0$ within each S subsystem (i.e. for DS=0 transitions only) was used instead. A fairly good agreement is obtained in the case shown, but as seen the quality is not the same for the three lines, the worst corresponding to the706 line (triplet system). Due to the strong contribution to this line from the 2^3S metastable and the relatively high population of that species under the conditions of the plasma periphery, the displacement of the maximum in the 706 line towards outer radii could be ascribed again to the lack of inclusion of the "memory effects" in our model. As seen, the model is able to reproduce the penetration of the He beam into the plasma within a reasonable accuracy. This would be expected from the lack of significant multi-step ionization processes and hot ion collisions under ECR heating conditions. Also shown is the effect of a ±10% error in the 728line intensity on the reconstructed profiles. Similar variations in these profiles are obtained by a change in the $3^1P \rightarrow 3^1S$ rate constant of ~30 % (not shown). As seen, higher ne values (as suggested in fig. 8 by the reflectometer signal, and arising from a decrease in the 728 line intensity) would still be compatible with the experimental profiles, but a deviation towards higher intensities at 728nm leads to a significant worsening of the fittings. By using the averaging possibilities of the high frequency operation, the technique could be used to assess the accuracy of the tabulated rate constants in a finer level.

A powerful tool for the study of the excited levels in the He beam is Laser Induced Fluorescence (LIF). This technique has already been used by several authors is hot plasmas and its use for electric field determination in plasmas in combination with a supersonic He beam has been proposed by Takiyama and co-workers [16]. The technique has already been employed at the Ciemat for sputtering measurements in deposition plasmas [17] and the same set-up it is now being installed in TJ-II, as schematically shown in figure 5. Several pumping/detection schemes are foreseen in the He beam diagnostic. Thus for example, pumping of the $2^1S \rightarrow 3^1P$ transition at 501.6 nm at moderate laser beam powers would instantaneously (~1ns) deplete the metastable population and transiently induce a strong increase in the population of the 3^1P level. These perturbations in the equilibrium distribution would propagate in a collision-relevant time scale (< 0.1ms) to other levels monitored for the diagnostic (i.e., 667nm emission from 3^1D and 728 nm from 3^1S), thus allowing the verification of the relevant rate constants involved in the model. Conversely, the laser can be used to selectively ionize some critical excited levels, in a similar way to that proposed for He exhaust measurements in ITER by LII [18]. A simple numerical estimate for the effect of the laser depletion of the metastable 2^1S level by either method in the populations of the singlet, n=3 levels is shown in Table I, for a constant electron density of 2.10^{18} m^{-3} and a broad range of Te values. As seen, a noticeable decrease in the 667 and 728 emission

intensities will follow the laser pulse (20 ns). Also, the decrease in the 501 nm line ($3^1P->2^1S$) shows a significant Te dependence at low temperature values. In this respect, the access to the excited levels by laser radiation could open the application of the diagnostic to temperature ranges typical for divertor operation, although this topic deserves a full discussion with inclusion of other atomic processes not considered in our C-R model. Work in this direction is presently in progress at the TJ-II.

Summary:

Conventional and new edge and plasma wall interaction diagnostics have been applied for the operation and confinement characterization in TJ-II. Particular effort is being devoted to the optimization of atomic beam diagnostics. From the beam source side, improvement in the Li oven design and in the He beam source has been achieved. A high repetition rate, pulsed supersonic He beam has been built. From the modeling point of view, checking of the self-consistency of the C-R model used for the He beam interpretation has been performed under some conditions. Direct testing of the model by perturbative LIF experiments are in preparation.

References.

[1] C. Alejaldre et al. 1999 Plasma Phys.Control.Fusion **41A** 539

[2] F. L. Tabarés et al, 2001 J.Nucl. Mater **290-293** 748

[3] D. Tafalla and F. L. Tabarés 2001 J.Nucl. Mater **290-293** 1195

[4] E. de la Cal et al. 2001 J. Nucl. Matter. **290-293** 579.

[5] B. Brañas et al. 2001 Rev. Sci. Instrum. **72** 602

[6] a) M. Brix, Proc. 1997 24th EPS Conference on Controlled Fusion and Plasma Physics, Berchtesgarden **21A** 1837, and references therein. b) ibid. 2002Workshop on He excitation data in plasmas, JET-EFDA, Culham, U.K., Feb.

[7] Y. Andrew and M G O´Mullane, 2000 Plasma Phys. Control. Fusion **42** 301

[8] F.L. Tabarés et al. 2001 Plasma Phys. Control. Fusion, **43** 1023.

[9] B. Zurro et al, 1993 Plasma Phys. Control. Fusion **35** 349

[10] M.A. Pedrosa et al. 1999 Rev. Sci. Instrum. **70** 415

[11] C.Hidalgo, private communication

[12] F.L. Tabarés, D. Tafalla, V. Herrero and I. Tanarro, J. Nucl. Mater. 1997 **241-243** 1228.

[13] T. Diez-Rojo, V. J. Herrero, I. Tanarro. 1997 Rev. Sci. Instrum **68** 1423.

[14] B. Schweer, G. Mank, A. Pospieszczyl, B. Brosda, B. Pohlmeyer. 1992 J. Nucl. Matter. **196-198** 174.

[15] L.C. Johnson and E. Hinnov. 1969 Phys. Rev **187** 143.

[16] K. Takiyama et al. Rev. Sci. Instrum.1997 **68** 1028.

[17] D. Tafalla et al. J.Nucl. Mater 1995 **220-222** 899.

[18] K. Uchino et al. 1996 "Laser Diagnostics of hydrogen and helium atoms in a divertor region", in *Diagnostics for Experimental Thermonuclear Fusion Reactors*, Plenum Press, N.Y. p.595

Table I: Relative population decrements for several excited states of He atoms upon complete depletion of the 2^1S metastable level in a plasmas, at $n_e = 2.10^{12}$ cm^{-3}

Level	Te = 4eV	Te = 10eV	Te = 20eV	Te = 40eV	Te = 60eV
2^1P	47%	30%	20%	14%	12%
3^1S	14%	11%	10%	9%	8%
3^1D	29%	28%	25%	22%	21%
3^1P	13%	7%	4%	3%	3%

Figures Captions:

Figure 1: Instrumented, graphite limiters with optimized shape. The dimensions along the toroidal (ϕ), radial(R) and vertical (z) directions are shown.

Figure 2: Correlation between the mass spectrometer signals of released He and the rate of density rise in the discharge.

Figure 3: Top. Scheme of the fast GIS in TJ-II.

Bottom. Typical traces of plasma start-up with fast gas injection.

Figure 4: Li beam set-up

Figure 5: He beam set-up

Figure 6: Top. Pulse shape of He lines without intermediate chamber.

Bottom. 200 Hz beam operation. 706 line intensity at several radial locations.

Figure 7: Electron density and temperature profiles from He beam diagnostic and: ne. reflectometer, (2 initialisations), Te: ECE and Langmuir probes for two wall scenarios (see text)

Figure 8: Self-Consistency Check of the He beam emission in TJ-II. The effect of a $\pm 10\%$ error in the intensity of the 728 in the reconstructed profiles and the in modelling of the profiles is shown.

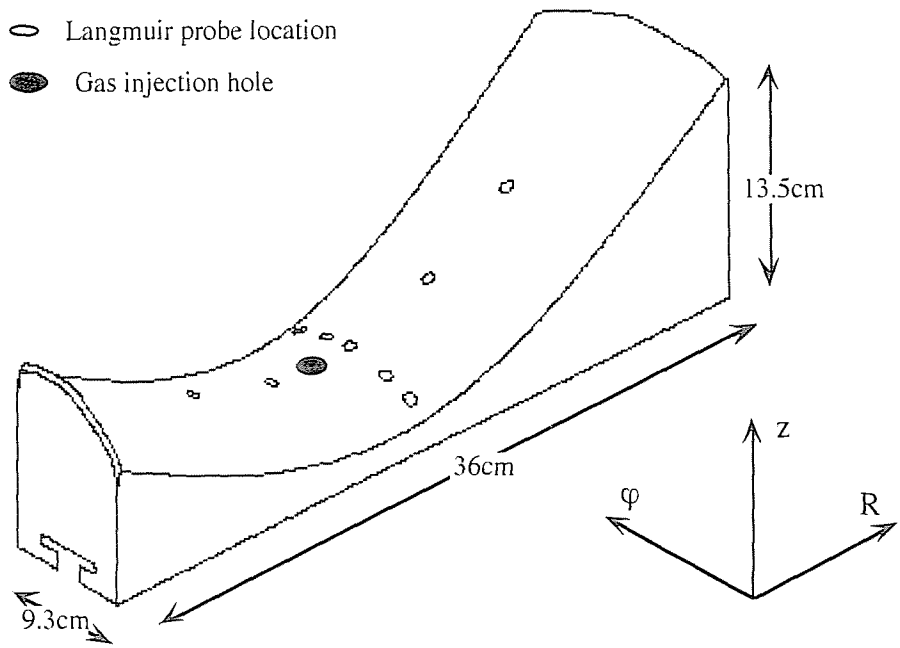

Figure 1.

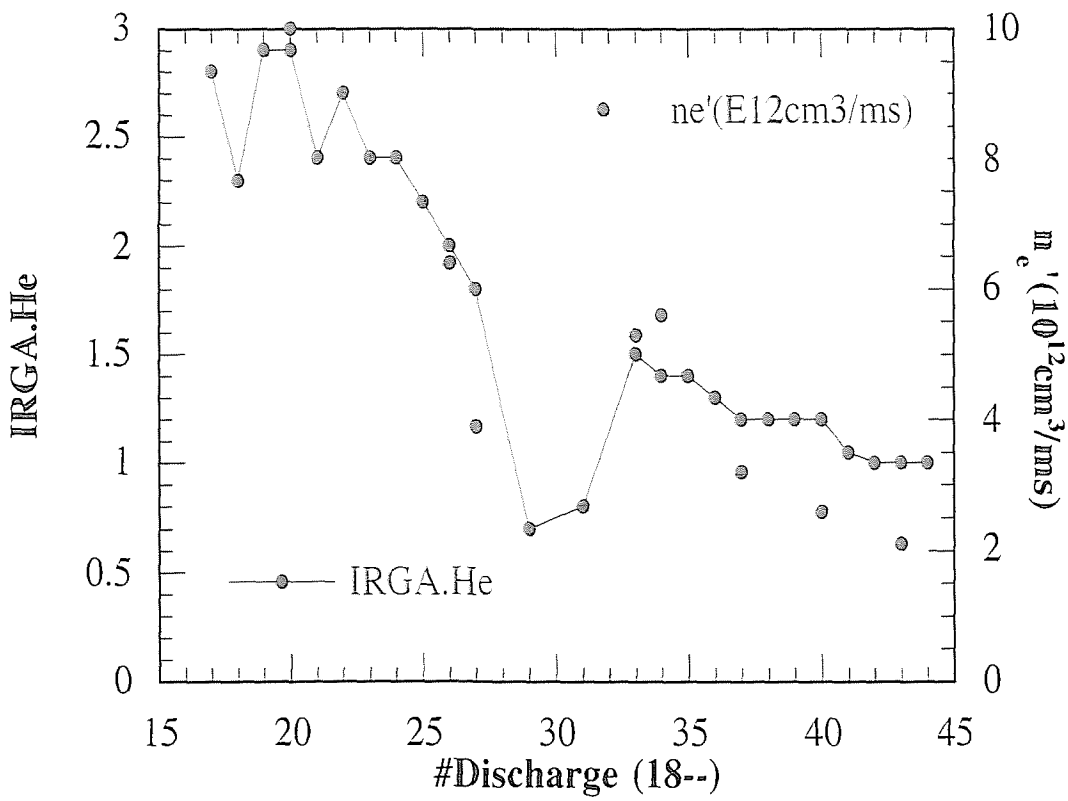

Figure 2

a)

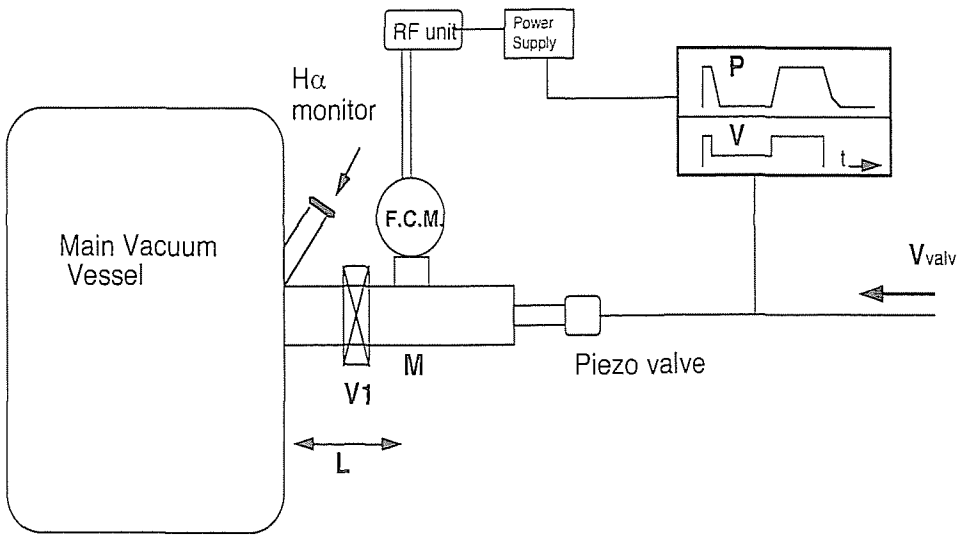

b)

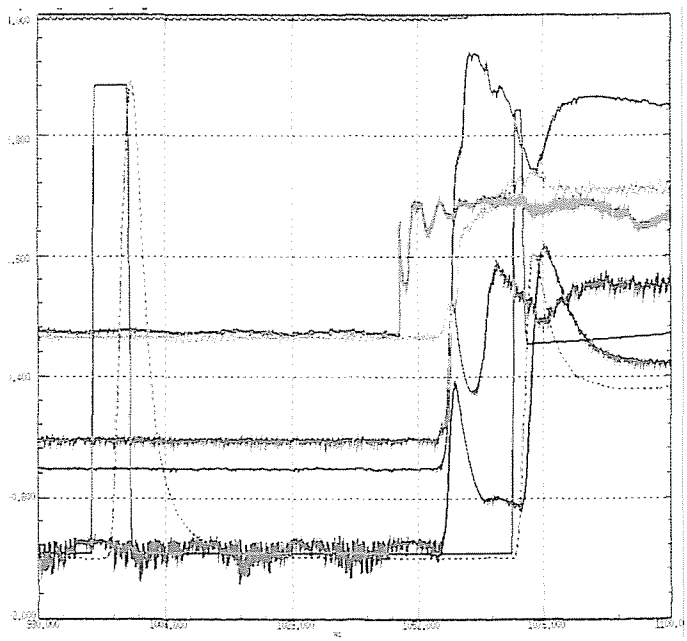

Electron density
Central Te
Gyrotron pulse
Limiter Hα
V_{valve} (square pulses)
Hα puffing
P baratron (dots)

Figure 3.

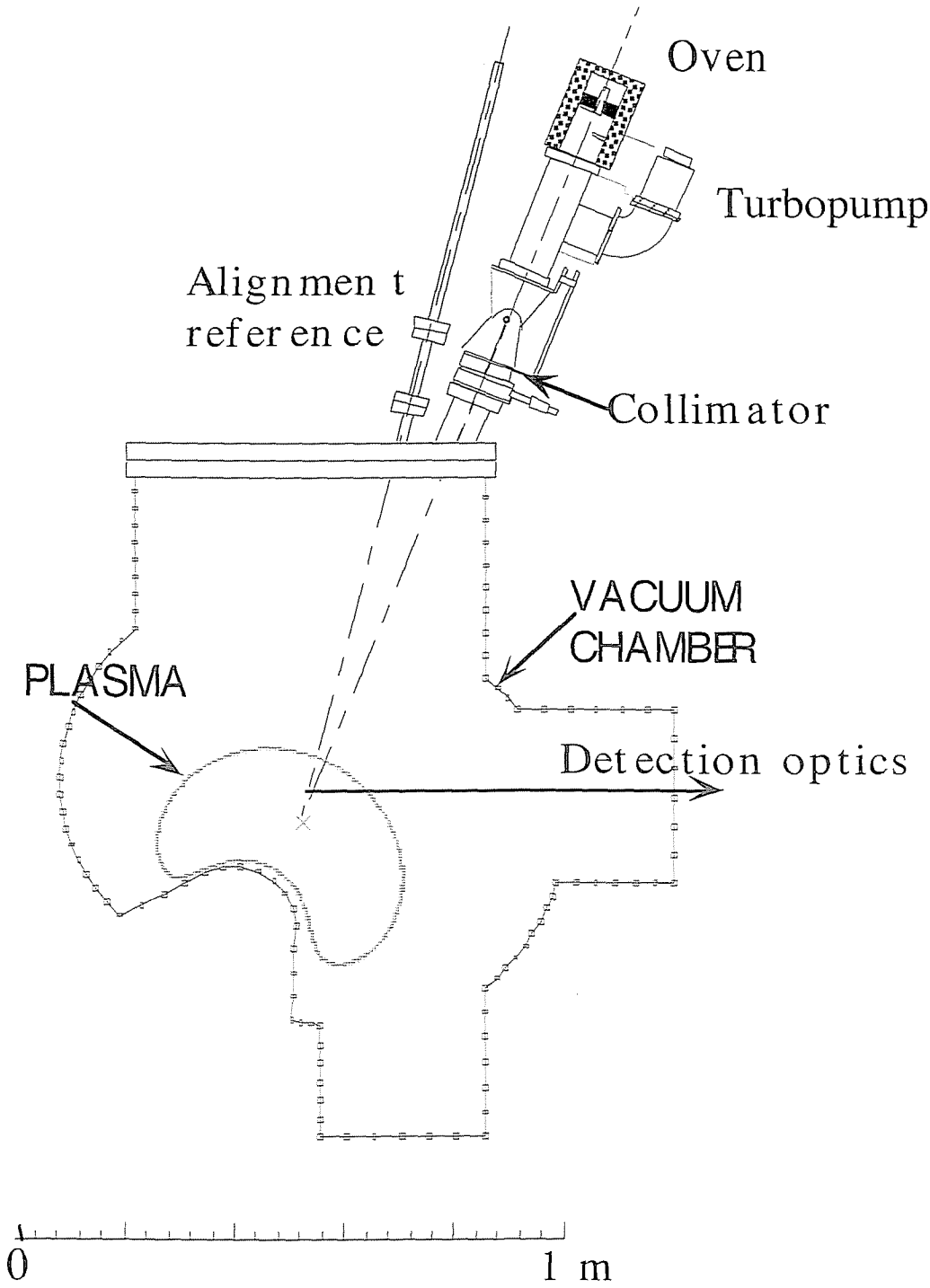
Oven
Turbopump
Alignmen t
refer en ce
Collimator
VACUUM
CHAMBER
PLASMA
Detection optics
0
1 m

Figure 4.

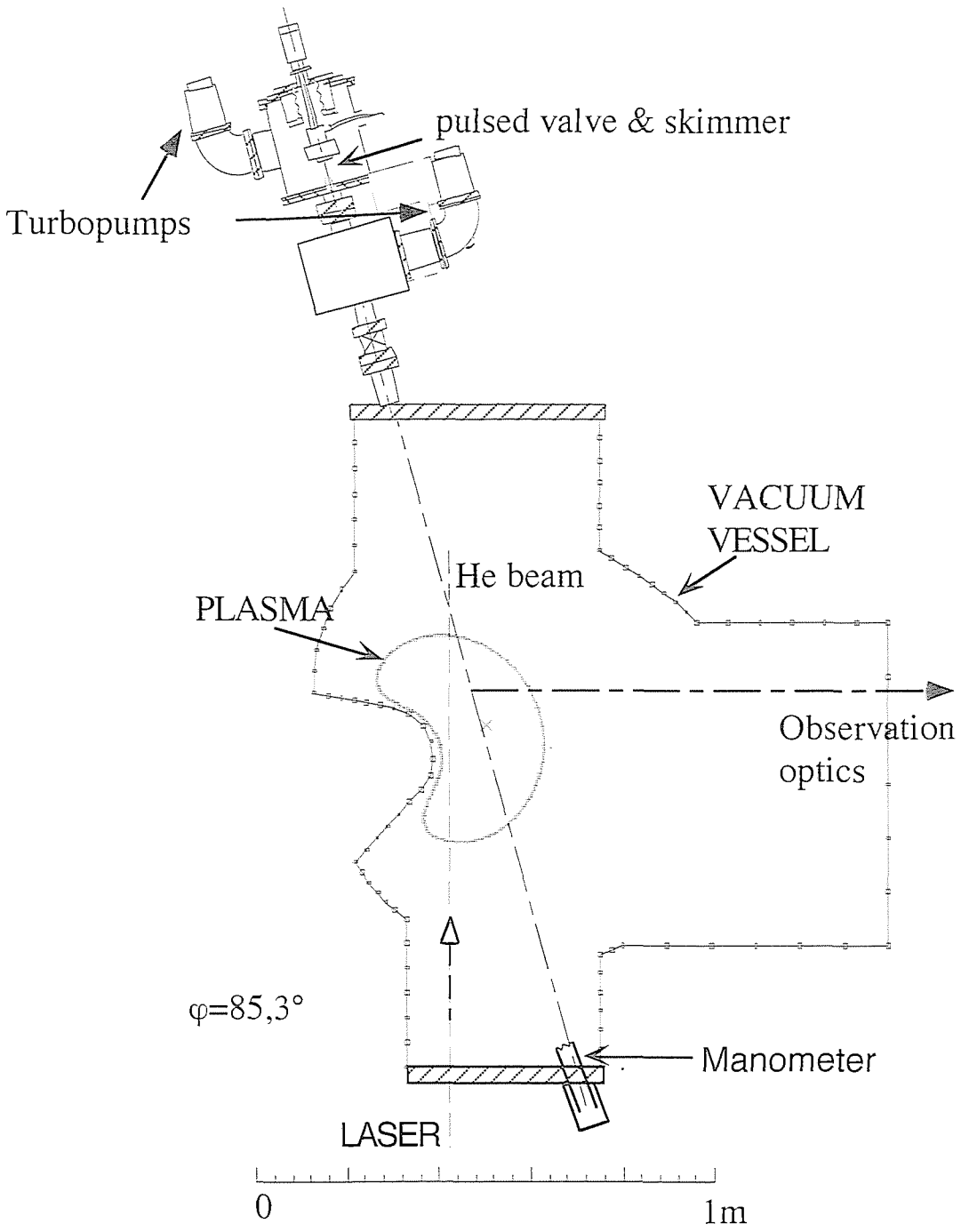
pulsed valve & skimmer
Turbopumps
VACUUM
VESSEL
He beam
PLASMA
Observation
optics
φ=85,3°
Manometer
LASER
0
1m

Figure 5.

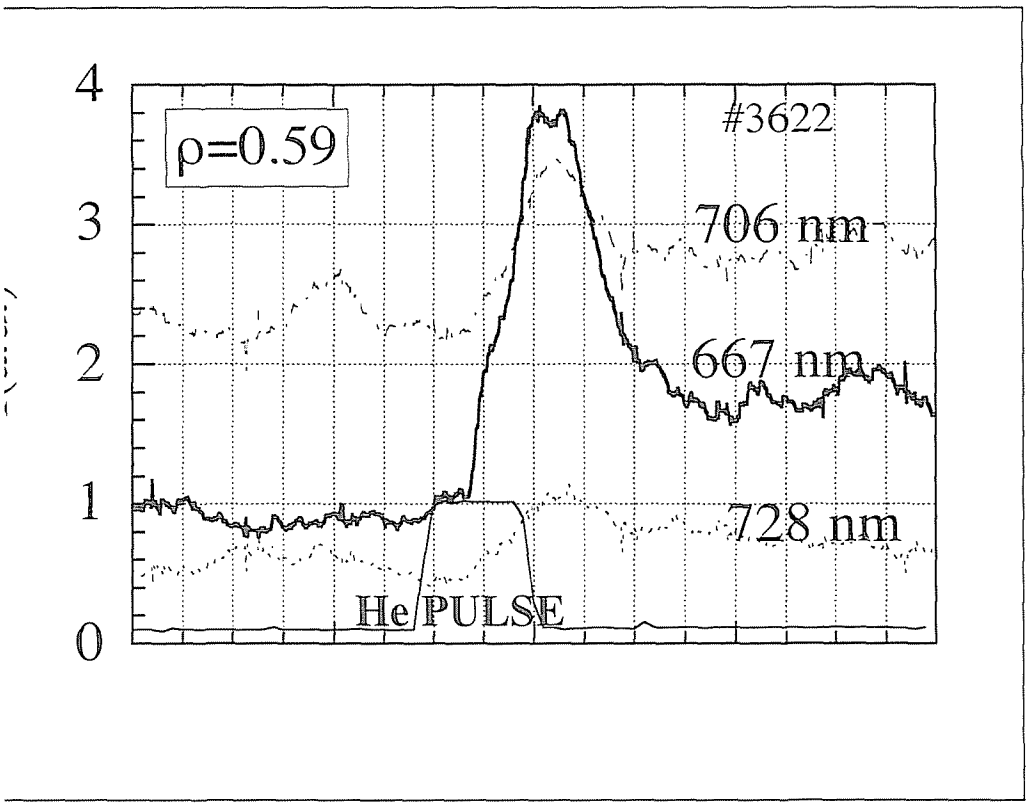
4
3
2
1
0
ρ=0.59
#3622
706 nm
667 nm
728 nm
He PULSE

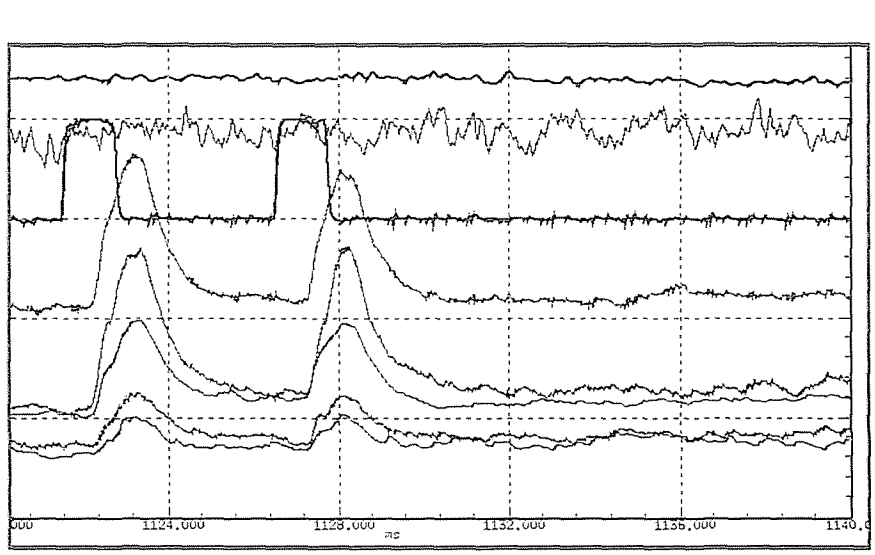
Ne
Hα
He
pulse
r/a
0.80
0.76
0.72
0.68
0.65
1124.000
1128.000
1132.000
1136.000

Figure 6.

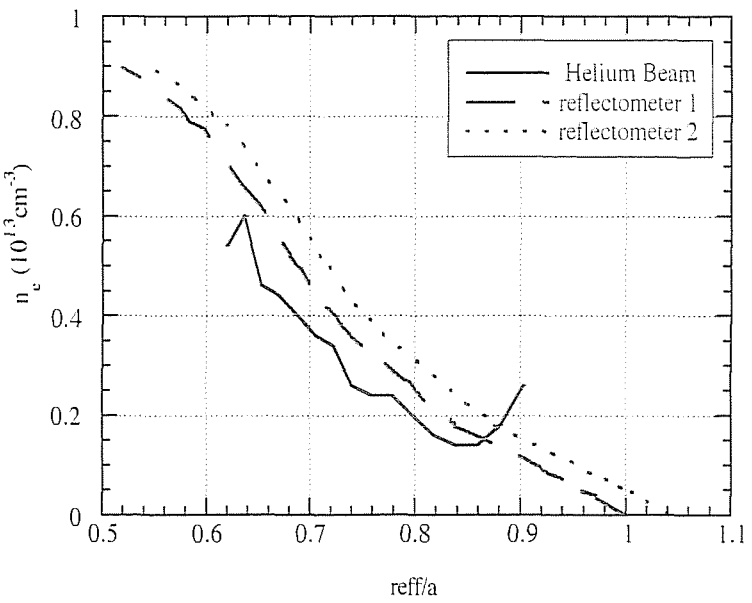
Helium Beam
reflectometer 1
reflectometer 2
n_e (10^{13}cm^{-3})
reff/a

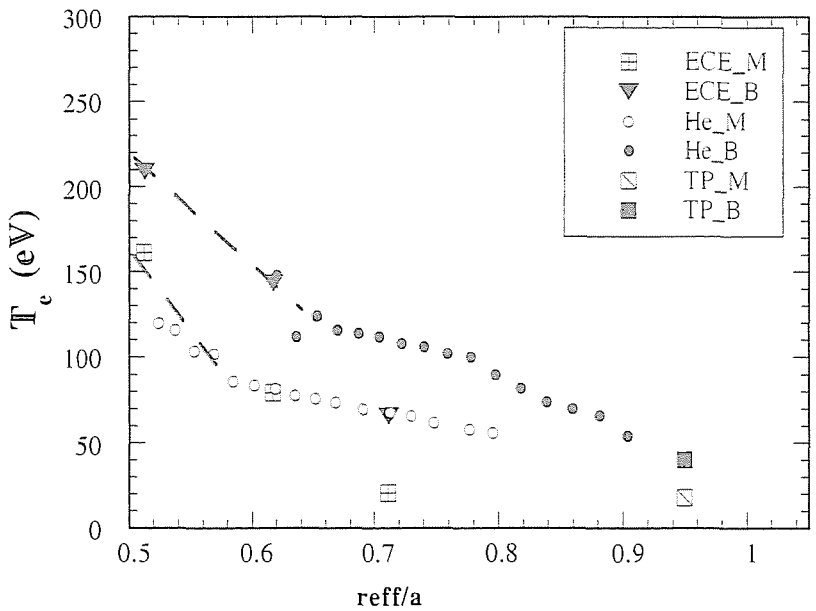
ECE_M
ECE_B
He_M
He_B
TP_M
TP_B
T_e (eV)
reff/a

Figure 7.

Figure 8.

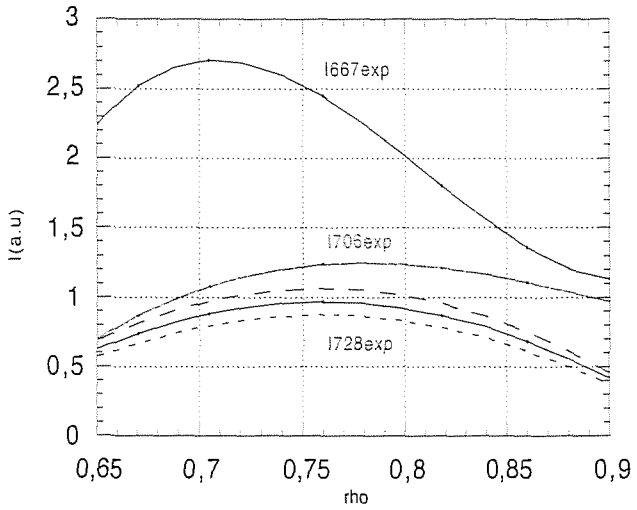
I667exp
I706exp
I728exp
I(a.u)
rho

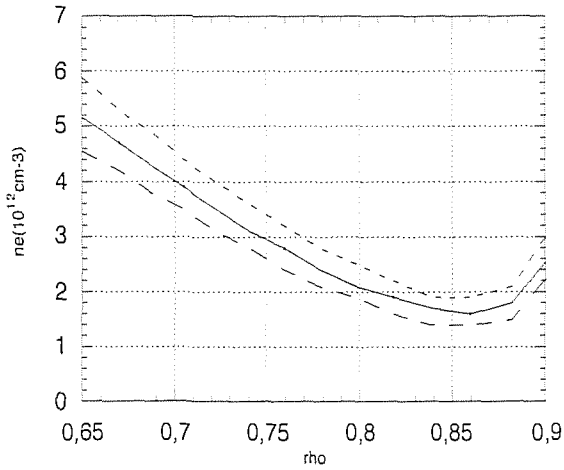
ne(10^12cm-3)
rho

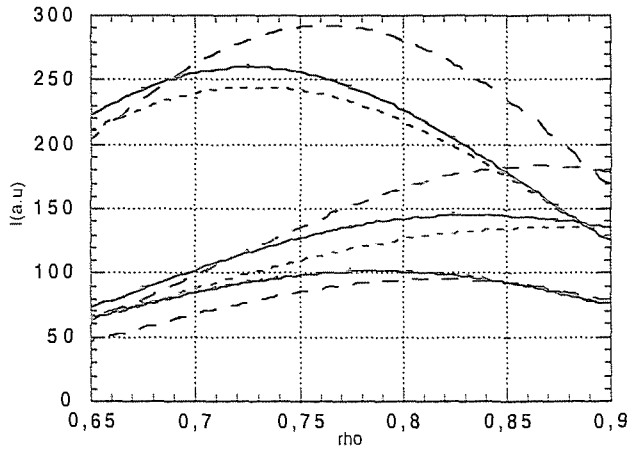
I(a.u)
rho

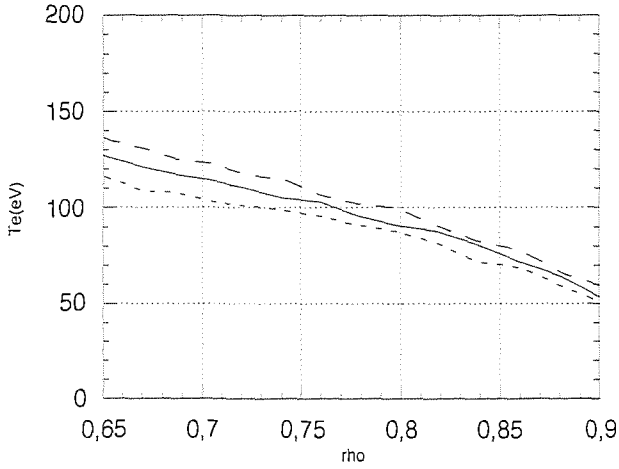
Te(eV)
rho